

05

Calculation of effective dielectric permittivity and electrical conductivity of composites containing conductive oriented filaments

© A.E. Postelga, S.V. Igonin

Saratov National Research State University,
410012 Saratov, Russia
e-mail: sanyalace@list.ru, igoninsemen@ya.ru

Received April 16, 2025

Revised May 31, 2025

Accepted July 1, 2025

A model has been developed for calculating the frequency dependence of the microwave reflectivity from composites with oriented fibers. The oriented fiber composite was replaced by a multilayer model, each layer of which was calculated using perturbation theory. The model was applied to calculate the effective complex permittivity of these composites. The feasibility of using this model to calculate the reflectivity spectrum from composites with nonuniform fillings was demonstrated. The applicability criteria for a simpler model in which the fiber composite is replaced by a lamellar structure were also examined.

Keywords: fiber composites, permittivity, electrical conductivity, microwave, threads, fibers, columns, effective medium, numerical methods, perturbation theory.

DOI: 10.61011/TP.2026.01.62845.62-25

Introduction

Modern composite dielectric materials [1] are very widely applied in some fields of science and technology due to the following advantages: a high strength/weight ratio [2], microwave radiation absorptivity [3], high thermal conductivity [4], breakdown strength [5], etc. Properties of this kind of the composites can be adapted according to specific requirements by changing a volume ratio and a configuration of components. Mechanical and electrical characteristics of the materials can be significantly improved when adding carbon or metal fibers [6,7]. In this regard, it is relevant to monitor electrophysical parameters of fiber composites.

There are numerous models of effective permittivity, among which models of Maxwell-Garnett [8], Landau-Lifshitz-Looyenga or Lihtenekker [9,10]. In most cases, approximate models are designed for calculating parameters of homogeneous composites with spherical inclusions. Non-sphericity is taken into account by introducing correction coefficients like, for example, in a Nielsen model, which was used by authors of the study [11] for describing properties of filled polymers. Approximately, the fibers can be accepted to be elongated ellipsoids. Then, taking into account a depolarizing factor, an effective medium theory (EMT) can be applied for calculating the fiber composites [12]. The study [13] proposes a simply semi-analytical-numerical method based on an averaging configuration method, a moment method and a Monte Carlo method, for obtaining effective properties of a thin composite plate with inclusions as uniformly distributed fibers. Fiber orientation was taken into account in the study [14].

The considered effective medium theories make it possible to calculate parameters of the homogeneous composites. Measurements made by microwave waveguide methods

make it possible to take into account heterogeneities. In case of the multi-layer composites, it is proposed to calculate effective permittivity by a general volume formula, but taking into account distribution of an electric field in a waveguide cross section [15].

Composites that are based on an epoxy resin, contain inclusions as thin threads of carbon nanotubes and a magnetic liquid and formed when drying in a magnetic field, were experimentally investigated in the study [16]. The effective parameters of the composite were determined by analyzing spectra of microwave reflection coefficients within the range 9 – 10 GHz from a periodic structure with a dislocation as the studied sample placed in the rectangular waveguide. The structures of this kind were named microwave photon crystals [17] and applied, in particular, when determining parameters of the materials [18]. Complex permittivity of the inclusions was determined by simulating a composite structure by a finite element method in the HFSS software program. It should be noted that with a decrease of the thickness of the threads a calculation time increases in several times, while with the thicknesses of less than 15 μm (which corresponds to several hundred threads in the sample) the calculation is very difficult.

The present study proposes a method of calculating effective permittivity and effective electrical conductance of the composites that contain various volume portions of filamentary inclusions („threads“) of micron thicknesses (below 200 μm). The method implies calculating the spectra of the microwave reflection coefficient of the periodic structure that is placed in a rectangular waveguide and contains the measured sample with oriented filamentary inclusions in a central layer. A distribution of threads along a direction of propagation of the microwave will be taken into account by dividing a portion of the waveguide

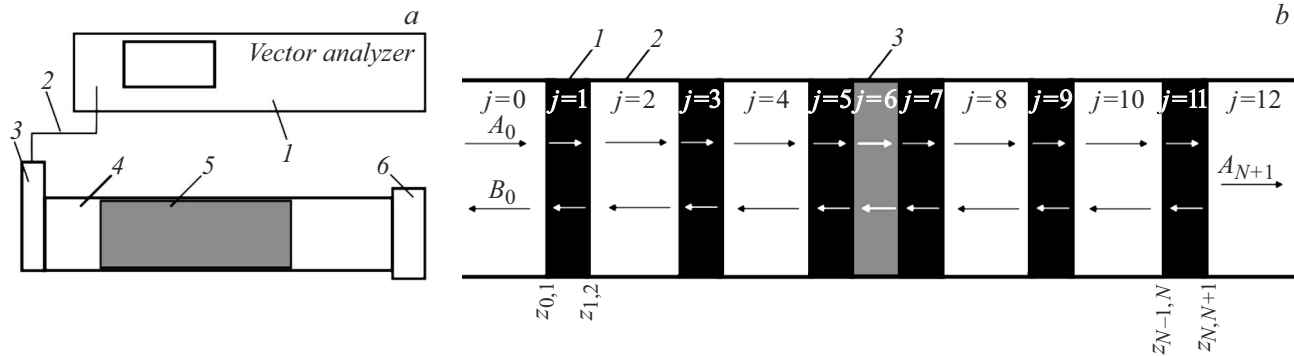


Figure 1. Schematic image of the experimental setup and the studied structure. *a* — the experimental setup: 1 — the vector network analyzer, 2 — the coaxial, 3 — the coaxial-wave transition, 4 — the rectangular waveguide, 5 — the studied structure, 6 — the concerted load; *b* — the studied structure: 1 — the polycore layers of the thickness of 0.97 mm, 2 — the fluoroplastic layers of the thickness of 8.95 mm, 3 — the studied sample of the thickness of 3.95 mm, j — the layer number, $z_{j,j+1}$ — a distance from the structure surface to a boundary between the layers with the number j and $j + 1$, A_j and B_j — amplitudes of incident and reflected electromagnetic waves in the layer with the number j .

containing the studied sample into many equally-thick layers. The threads in the waveguide cross section will be taken into account using a perturbation theory method, which was successfully applied for refining parameters of the magnetic liquid by taking into account agglomerates of magnetic nanoparticles in the experimental study [19]. By the obtained spectrum, solving a two-parameter inverse problem will result in determining a real part of permittivity and electrical conductance of the composite.

Derivation of relationships that determine effective permittivity is based on using a solution of the problem of polarization of a selected model of an „effective diffuser“ placed in the homogeneous external field [8]. At the same time, the effective medium theories do not allow taking into account the thread spatial distribution, whose influence increases when the number of the threads per a unit area decreases. The proposed method of calculation of the electrophysical parameters makes it possible to take into account the thread spatial distribution and can be applied for analyzing structures with an arbitrary predefined spatial distribution of oriented threads and not only for the homogeneous composites. The method being developed will be used for determining the parameters of the inclusions of the real composites and explaining the spectra of the microwave reflection coefficient in case of heterogeneous filling [16].

The proposed calculation method can be applied when solving a various kind of problems that are related to analysis of propagation of the microwave in an anisotropic waveguide.

1. Performing and simulating the experiment

A diagram of the experimental setup is shown in Fig. 1, *a*. The incident microwave from the vector analyzer 1 was directed along the coaxial 2 via the coaxial-wave transition 3

into the waveguide 4 with the section 23×10 mm, in which the studied structure was placed 5. Microwave power transmitted through the structure was absorbed by the concerted load 6 and the reflected wave returned into the vector analyzer 1 via the coaxial-wave transition 3 along the coaxial 2. The measurements were performed using the vector network analyzer Agilent Tech. 5242A PNA-X Network Analyzer within the frequency range 9 – 10 GHz.

We have studied the frequency dependences of the TE_{10} -type microwave reflection coefficient of the photon crystal (Fig. 1, *b*), which is alternating layers of polycore of the thickness of 0.97 mm and fluoroplastic of the thickness of 8.95 mm (11 layers altogether). Instead of fluoroplastic, the sixth layer included the studied sample, which was the dislocation of periodicity of the photon crystal. The studied samples were shaped as parallelepipeds of the size $23.00 \times 10.00 \times 3.95$ mm and were a composite „material epoxy resin — magnetic liquid — carbon nanotubes“ (ER/ML/CNT) with a CNT weight portion of 0.053 % and a CNT weight/ML weight ratio of 0.02. The samples were solidified during one day at the various values and directions of induction of the magnetic field. The parameters of the photon crystal and the dislocated layer were selected so that a reflection coefficient minimum in a band gap of the photon crystal was in an X-range used in radio detecting and ranging, ground and satellite radio communication and was quite sharp to allow investigating anisotropy of properties of the filamentary inclusions at a low volume portion. It should be noted that other parameters being equal, variation of the thickness of the dislocated layer results in a shift of a reflection coefficient minimum and variation of resonance Q factor, which may result in variation of accuracy of determination of the parameters as well.

The TE_{10} -type wave belongs to transverse electric waves, for which strength of the electric field has a component that is only perpendicular to the direction of propagation of the microwave. Components of the electric and magnetic fields E_m and H_m of the TE_{10} -type wave, in which the electrical

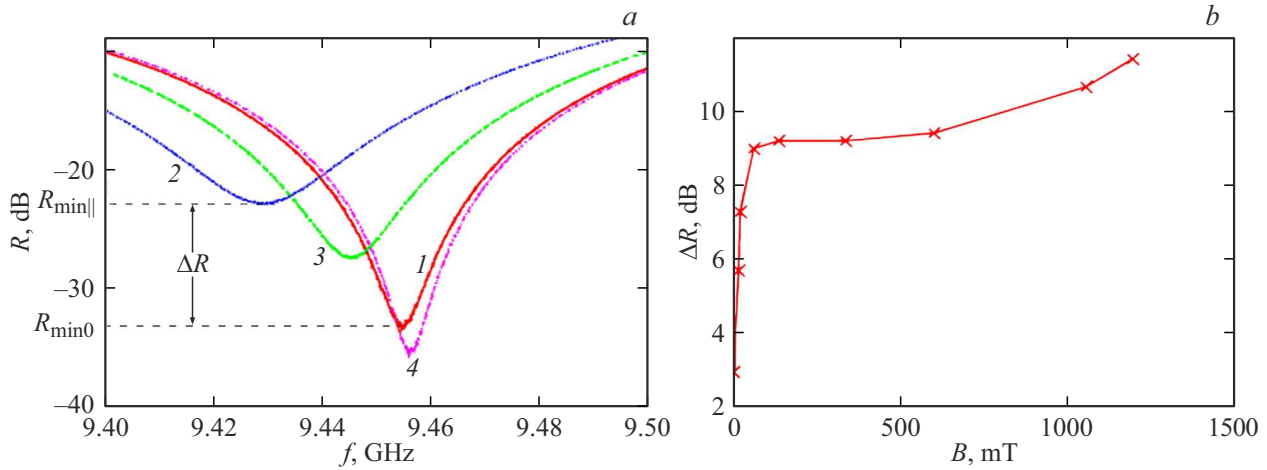


Figure 2. Experimentally measured dependences: *a* — of the reflection coefficient of the microwave on the frequency, the dislocation is provided by the samples dried at the magnetic field with induction of 130 mT, which was oriented: 1 — without the magnetic field, 2 — parallel, 3 — at the angle of 45° , 4 — perpendicular to the electrical component of the microwave (to the wide wall of the waveguide), $\Delta R = R_{\min ||} - R_0$ — a difference of minimums of the reflection coefficient when the structure has the sample dried in the magnetic field that was parallel to the narrow wall of the waveguide, and without the magnetic field; *b* differences of the minimums of the reflection coefficient ΔR on a value of induction of the magnetic field, at which the samples were manufactured.

component is parallel to a narrow wall of the waveguide (to the axis Y), are pre-defined by the known relationships

$$E_y(x, \omega) = -\frac{\omega\pi}{a} \sin\left(\frac{\pi x}{a}\right),$$

$$H_x(x, \omega) = -\frac{\sqrt{-1} \cdot \gamma_m(\omega) \cdot \pi}{\mu\mu_0 a} \sin\left(\frac{\pi x}{a}\right),$$

$$H_z(x, \omega) = -\frac{\sqrt{-1} \cdot \pi^2}{\mu\mu_0 a^2} \cos\left(\frac{\pi x}{a}\right),$$

$$E_x = H_y = E_z = 0,$$

where γ_m and μ is a constant of propagation and permeability in the considered portion of the waveguide, a is a size of a wide wall of the waveguide, μ_0 is a magnetic constant, ω is an angular frequency of the microwave.

Dislocation of periodicity of the structure of the photon crystal results in a typical sharp reflection coefficient minimum on the frequency dependence (Fig. 2, *a*). A position of the minimum by the frequency and the value is determined by parameters of the studied sample. Placing as the dislocation of periodicity the sample dried in the magnetic field with an induction vector directed parallel to the electrical component of the microwave in the waveguide results in reduction of the reflection coefficient and shifting of the minimum to the left (Fig. 2, *a*, the curve 2) relative to the sample dried without the magnetic field (Fig. 2, *a*, the curve 1). It indicates the increase of conductivity and permittivity of the sample, which is caused by appearance of elongated structures of CNT and the magnetic particles along the direction of the magnetic field. When the angle between the magnetic field and the electrical component of the microwave increases, the reflection coefficient decreases (Fig. 2, *a*, the curve 3), while

with a perpendicular orientation it is even less than for the sample dried without the magnetic field (Fig. 2, *a*, the curve 4).

Orientation of the elongated structures parallel to the narrow wall of the waveguide results in maximum interaction of the electrical component of the microwave with them. The sharp increase of the value of the reflection coefficient minimum with an increase of induction of the magnetic field (Fig. 2, *b*) is related formation of the elongated threads at the small magnetic fields starting from 5 mT. A process of structure formation in the composite reaches saturation with the value of magnetic induction being 100 – 500 mT, the samples with the same parameters are produced. At the strong fields exceeding 600 mT, a ML-CNT suspension is contracted closer to the sample center, where the electrical field of the microwave is maximal. Correspondingly, interaction of the electromagnetic wave with the CNT structures enhances and the reflection coefficient increases.

The experiment was simulated in the electrodynamic 3D-simulation Ansys HFSS software program (Fig. 3). The studied samples were a composite material of epoxy resin with inclusions of conductive threads. The volume portion of the inclusions varied in the model from 0.1% to 10%. Coordinates of the inclusions were pre-defined by a random uniform distribution, for which a script was designed in a Visual Basic Script language. We have investigated a dependence of the reflection coefficient minimum of the TE_{10} -type microwave on the thickness, the volume portion, the real part of permittivity and electrical conductance of the inclusions. It was calculated with parallel and perpendicular orientations of the threads relative to the electrical component of the TE_{10} -type wave (to the axis Y).

The photon crystal is used due to a high degree of sensitivity of these structures to the parameters of the dislo-

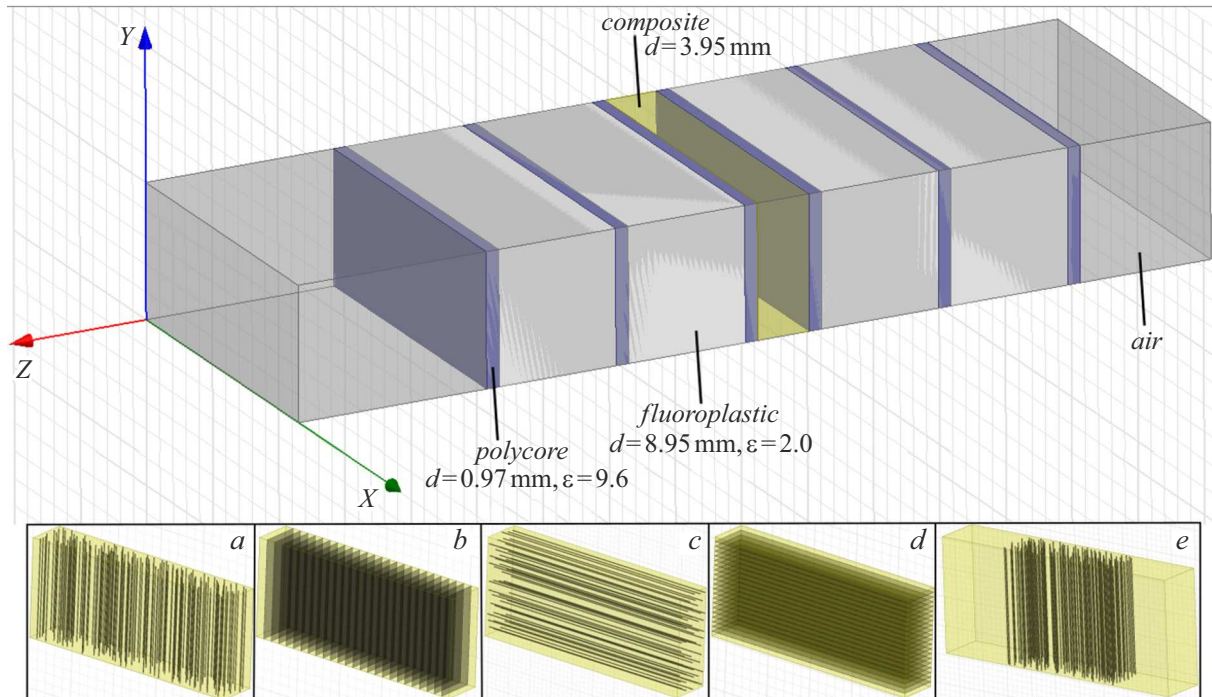


Figure 3. Studied periodic eleven-layer structure with the dislocated central layer which is the composite: *a, b* — with the threads and plates, which are oriented parallel to the narrow wall of the waveguide (to the axis *Y*); *c, d* — with the threads and plates, which are oriented parallel to the wide wall of the waveguide (to the axis *X*); *e* — with a heterogeneous distribution — the threads are shifted closer to the center.

cated layer, which makes it possible to increase accuracy when processing the experimental data. It is especially important when investigating the composites with a low volume portion of the inclusions or with parameters of the inclusions, which are slightly different from parameters of a matrix material.

2. Determination of the ML parameters

Before starting to theoretically describe the model, we will consider an experimental study for determination of the ML parameters. It demonstrates applicability of the multi-layer model for analysis of the structures containing the elongated oriented inclusions using the perturbation theory and a transfer matrix method.

The ML is a homogeneous suspension of single-domain nanoparticles of a ferro- or ferrimagnetic in water or organic solvent, which are stabilized by a surfactant. Interaction of electromagnetic radiation in the microwave range with the ML is described by a theory of dynamic magnetization of a single-domain particle in the internal field of anisotropy and an external magnetizing field. When reaching a threshold value of induction of the magnetic field of 2.5 mT, agglomerates are formed from the magnetic nanoparticles in the ML with the nanoscale particles and sizes of these agglomerates can be determined using means of optical microscopy.

Taking into account presence of the agglomerates shall result in a more exact theoretical description of interaction of the ML with the electromagnetic wave of the microwave range and, therefore, to an increase of accuracy of determination of the parameters.

The reflection coefficient of microwave electromagnetic radiation was measured using a bridge method by means of a double waveguide tee, whose measurement arm included an ML layer that fully filled the waveguide cross section. A principal diagram of a radio-interference setup used for the measurements is shown in Fig. 4. A signal source was a microwave sweep oscillator of the 8 mm range *1*, which was included via a gate *2* into the *H*-arm of the double waveguide tee *3*. Power of the signal supplied into the *H*-arm of the tee was controlled by means of the semiconductor microwave diode *4* installed in this arm. As a result of interference of waves reflected from a load in a support arm and the ML layer *5* in the measurement arm, which is placed between two thin dielectric wafers that are „transparent“ for microwave electromagnetic radiation and prevent spread of the ML along the waveguide, the *E*-arm of the double waveguide tee forms a difference microwave signal. In order to adjust phases and values of the amplitudes of the interfering signals, the support and measurement arms of the double waveguide tee include movable short-circuiting pistons *6, 8* and an attenuator *7*. The signal detected by means of the microwave diode *9*

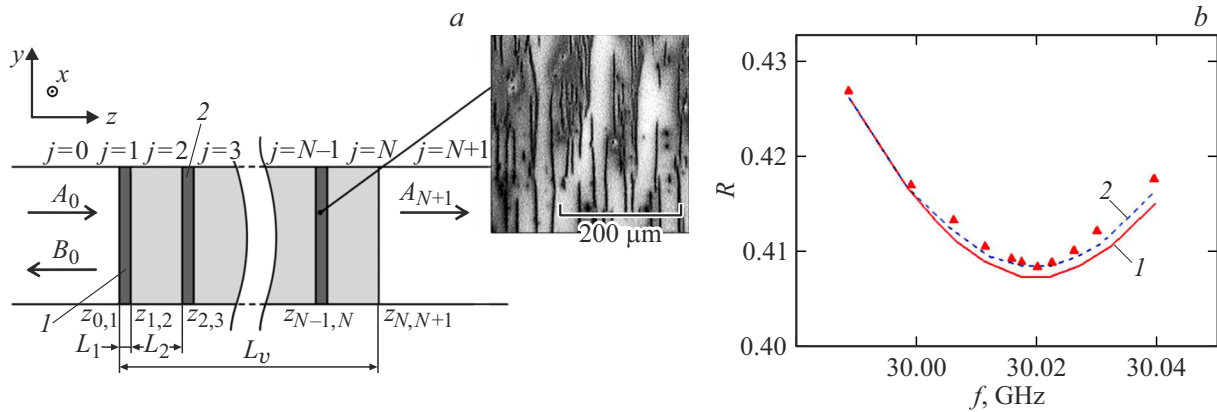


Figure 5. Agglomerated-ML model and results of the calculations: *a* — the structure of alternating layers of the ML unperturbed and perturbed by the agglomerates, which is used when calculating the frequency dependence of the reflection coefficient by means of the transfer matrix method: *1* — the portion of the agglomerated-ML waveguide, *2* — the portion of the waveguide with the unagglomerated magnetic liquid; *b* — the frequency dependences of the reflection coefficient of the ML layer at the temperature of 293 K, experimental dots are marked by triangles: *1* — the frequency dependence without taking into account the agglomerates, *2* — the frequency dependence with taking into account the agglomerates distributed across the ML volume.

Table 1. ML parameters calculated without/with taking into account agglomerates

Parameter	x_0	x_1	Δ , %
d , nm	8	8.28	3.5
φ	0.144	0.135	6.3
ε	3.58	3.19	10.9
$\text{tg } \delta$	0.045	0.052	15.5

of calculation sorts out the coordinates from left to right, then $z_n = z_{n+1} - d_{n+1}$, where z_{n+1} is a coordinate of the left boundary of the layer that is adjacent to n -layer to the left, d_{n+1} is its thickness.

Portions, in which the parameters and thicknesses of the layers are periodically repeated, will be written as a periodic group:

$$\underbrace{\alpha|\beta}_{z_i \Pi_i^4} = \underbrace{\alpha}_{z_i S_4} \underbrace{\beta}_{z_i - a S_3} \underbrace{\alpha}_{z_i - a - b S_2} \underbrace{\beta}_{z_i - 2a - b S_1}. \quad (2)$$

The right upper index 4 means a total number of the alternating layers of the thickness a and b with the parameters α and β . The lower index i is equal to a number of the layer as part of an embracing structure, in which the periodic group is, while the upper left index z_i is a coordinate of the left boundary of the periodic group as part of the embracing structure.

We use $\underbrace{\alpha_j}_{z_i U_i^n}$ to designate the nonperiodic group of n -layers with the various thicknesses d_j and parameters α_j ,

and extreme layers to the right and left in this structure have parameters α_1 and α_n , respectively. The group's total thickness d_u is designated in the lower grouping sign.

Then, using designations of the periodic groups (2) the pattern of the photon crystal (1) has a compact form

$$\underbrace{\text{air}}_{X_2} \underbrace{\alpha_1}_{z_1 U_1^{11}} \underbrace{\text{air}}_{X_0} = \underbrace{\text{air}}_{X_6} \underbrace{p|f}_{z_5 \Pi_5^4} \underbrace{p}_{z_4 S_4} \underbrace{\text{comp}}_{z_3 D_3} \underbrace{p}_{z_2 S_2} \underbrace{f|p}_{z_1 \Pi_1^4} \underbrace{\text{air}}_{z_0 X_0} <, \quad (3)$$

where d_{pc} is a thickness of the photon crystal.

3.2. Calculation of the reflection coefficient of the periodic structure

Propagation of the wave in the waveguide through the periodic structure is described by the transfer matrix method [17]. The following expression for components of the transfer matrix can be written:

$$\mathbf{T}^{(j)} = \mathbf{T}^{(j)}(z_j, \gamma_{j+1}, \gamma_j) = \begin{pmatrix} \frac{\gamma_{j+1} + \gamma_j}{2\gamma_{j+1}} e^{(\gamma_{j+1} - \gamma_j)z_j} & \frac{\gamma_{j+1} - \gamma_j}{2\gamma_{j+1}} e^{(\gamma_{j+1} + \gamma_j)z_j} \\ \frac{\gamma_{j+1} - \gamma_j}{2\gamma_{j+1}} e^{-(\gamma_{j+1} + \gamma_j)z_j} & \frac{\gamma_{j+1} + \gamma_j}{2\gamma_{j+1}} e^{-(\gamma_{j+1} - \gamma_j)z_j} \end{pmatrix},$$

which relates the coefficients A_j , B_j and A_{j+1} , B_{j+1} , which determine amplitudes of incident and reflected waves on both sides of the coordinate z_j (the left boundary of the layer of the number j), with a relationship

$$\begin{pmatrix} A_{j+1} \\ B_{j+1} \end{pmatrix} = \mathbf{T}^{(j)} \begin{pmatrix} A_j \\ B_j \end{pmatrix}, \quad (4)$$

$$\gamma_0^2 = \frac{\pi^2}{a_{wg}^2} - \omega^2 \varepsilon_0 \mu_0, \quad \gamma_j^2 = \frac{\pi^2}{a_{wg}^2} - \omega^2 \varepsilon_0 \mu_0 \varepsilon_j \mu_j, \quad (5)$$

where γ_0 and γ_j — electromagnetic wave propagation constants (along the axis Z) in vacuum and in the layer of the number j ; a_{wg} is a size of the wide wall of the waveguide; ω is a frequency of electromagnetic radiation; ε_0 and μ_0 are electric and magnetic constants; ε_j and μ_j are permittivity and permeability of the layer of the number j ; A_j, B_j are coefficients that determine amplitudes of the incident and the reflected wave from the layer of the number j ; z_j is a distance from the structure surface, which is counted along the direction of propagation of the electromagnetic wave.

Coefficients A_{N+1} and B_0 that determine amplitudes of the wave transmitted through the multi-layer structure and the wave reflected therefrom are related to a coefficient A_0 that determines an amplitude of the incident wave by the following relationship:

$$\begin{pmatrix} A_{N+1} \\ 0 \end{pmatrix} = \mathbf{T}_N \begin{pmatrix} A_0 \\ B_0 \end{pmatrix},$$

where $\mathbf{T}_N = \begin{pmatrix} \mathbf{T}_N[1, 1] & \mathbf{T}_N[1, 2] \\ \mathbf{T}_N[2, 1] & \mathbf{T}_N[2, 2] \end{pmatrix} = \prod_{j=N}^0 \mathbf{T}^{(j)}$ — a transfer matrix of the periodic structure consisting of N -layers.

Writing the reflection coefficient $R = B_0/A_0$ via elements of the transfer matrix \mathbf{T}_N according to the relationship (4), we obtain

$$R = -\frac{\mathbf{T}_N[2, 1]}{\mathbf{T}_N[2, 2]}. \quad (6)$$

3.3. Example of composing the transfer matrix using the introduced designations

We compose the transfer matrix \mathbf{T}_N for the photon crystal (Fig. 3) with the dislocated layer as the studied composite:

$$\begin{array}{cccccccccccc} \overbrace{X}^{air} & \overbrace{S_{11}}^p & \overbrace{S_{10}}^f & \overbrace{S_9}^p & \overbrace{S_8}^f & \overbrace{S_7}^p & \overbrace{D_6}^{comp} & \overbrace{S_5}^p & \overbrace{S_4}^f & \overbrace{S_3}^p & & \\ \infty & d_1 & d_2 & d_1 & d_2 & d_1 & d_{comp} & d_1 & d_2 & d_1 & & \\ \overbrace{S_2}^f & \overbrace{S_1}^p & \overbrace{X}^{air} & & & & & & & & & \\ d_2 & d_1 & \infty & & & & & & & & & \end{array} < .$$

For each boundary we write the transfer matrix between the left layer and the right layer. For example, for the left

boundary of the layer of the number 6 — $\overbrace{S_7}^p \left| \overbrace{D_6}^{comp} \right._{d_{comp}}$ — the

transfer matrix will be written as $\mathbf{T}^{(6)}(z_7 - d_1, \gamma_p, \gamma_{comp})$, where the coordinate $z_6 = z_7 - d_1$ is calculated as a coordinate of the left boundary of the seventh layer with subtraction of the thickness of the seventh layer. By multiplying the transfer matrices through all the boundaries of the periodic structure starting from the most left, we obtain a transfer matrix through all the periodic structure

consisting of 11 layers:

$$\begin{aligned} \mathbf{T}_{11} &= \mathbf{T}^{(11)}(z_{11}, \gamma_{air}, \gamma_p) \cdot \mathbf{T}^{(10)}(z_{11} - d_1, \gamma_p, \gamma_f) \\ &\times \mathbf{T}^{(9)}(z_{10} - d_2, \gamma_f, \gamma_p) \cdot \mathbf{T}^{(8)}(z_9 - d_1, \gamma_p, \gamma_f) \\ &\times \mathbf{T}^{(7)}(z_8 - d_2, \gamma_f, \gamma_p) \cdot \mathbf{T}^{(6)}(z_7 - d_1, \gamma_p, \gamma_{comp}) \\ &\times \mathbf{T}^{(5)}(z_6 - d_{comp}, \gamma_{comp}, \gamma_p) \cdot \mathbf{T}^{(4)}(z_5 - d_1, \gamma_p, \gamma_f) \\ &\times \mathbf{T}^{(3)}(z_4 - d_2, \gamma_f, \gamma_p) \cdot \mathbf{T}^{(2)}(z_3 - d_1, \gamma_p, \gamma_f) \\ &\times \mathbf{T}^{(1)}(z_2 - d_2, \gamma_f, \gamma_p) \cdot \mathbf{T}^{(0)}(z_1 - d_1, \gamma_p, \gamma_{air}) \\ &= \mathbf{T}^{(11)}(z_{11}, \gamma_{air}, \gamma_p) \cdot \prod_{i=10}^0 \mathbf{T}^{(i)}(z_{i+1} - d_{i+1}, \gamma_{i+1}, \gamma_i), \end{aligned} \quad (7)$$

where $z_{11} = z_0 + 6 \cdot d_1 + 4 \cdot d_2 + d_{comp}$.

Substituting (7) into (6), one can determine the reflection coefficient for a pre-defined frequency of the microwave (the frequency is included in a final formula through the expressions (5)). By sorting out the frequencies in a required range with a certain step, one can construct a spectrum of the microwave reflection coefficient of the photon structure.

4. Model of „many perturbation layers“ (MPL)

A shift of the minimum in the spectrum of the reflection coefficient of the photon crystal is determined by complex permittivity of the dislocated layer, which depends on electrophysical parameters of the inclusions, their geometric sizes and distribution across a sample volume.

Let us consider the sample of the composite material of the size $23.00 \times 10.00 \times 3.95$ mm, in which the threads of an equal thickness d_c are oriented in a carrier matrix parallel to the narrow wall of the waveguide along the axis Y (Fig. 3, *a*), i.e. parallel to the electrical component of the TE_{10} -type microwave. The coordinates of the threads in the plane XZ are pre-defined as per a random uniform distribution.

We develop a model that allows replacing this kind of the composites with a multi-layer structure. The parameters of each layer will be determined using an apparatus of the perturbation theory. For brevity, the below-described calculation method will be named by us as a model of „many perturbation layers“ (MPL). It should be noted that application of the model being developed is difficult in case of perpendicular orientation of the threads of the electrical component of the microwave (Fig. 3, *c*), which will be discussed with more details below (at the end of Section 4.2).

4.1. Taking into account a distribution of the inclusions along the axis Z

In order to take into account a distribution of threads along the direction of propagation of the microwave (the

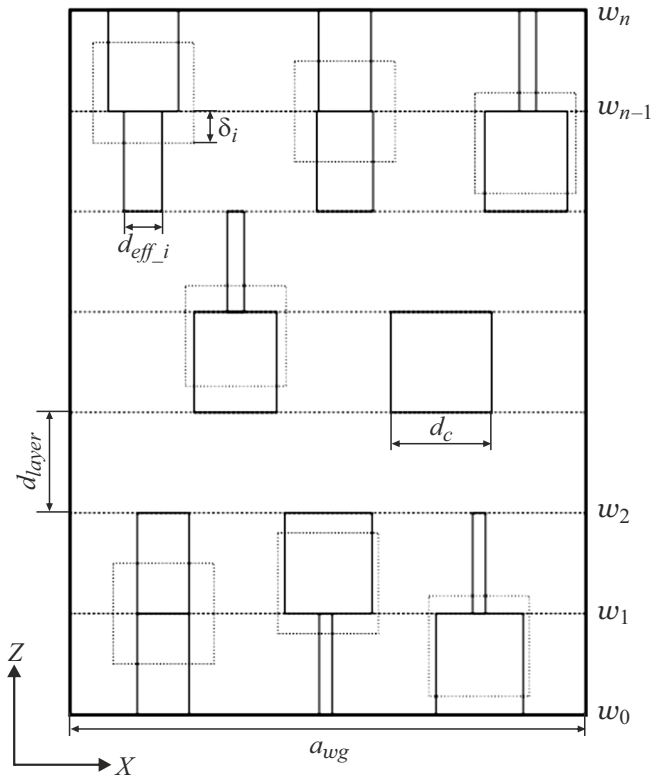


Figure 6. Distribution of threads in the plane XZ (the longitudinal section of the waveguide): dashed squares are threads in the real composite; dashed horizontal lines are boundaries of the layers of the multi-layer mode; rectangles marked by solid lines are threads produced by pre-defining an effective width and used in the model.

axis Z), we divide the composite into equal layers of the width d_c . There will be $n = \text{ceil}\left(\frac{d_{comp}}{d_c}\right)$ in total, where ceil is an upward rounding function. The vast majority of the threads (Fig. 6 — the dashed squares) will be at the boundary (Fig. 6 — the dashed lines) of one of the layers. We replace a part of the thread volume in the layer with an inclusion as a parallelepiped of the sample volume (Fig. 6 — rectangles marked by the solid lines). Sizes of the parallelepiped along the axes Y and Z coincide with the respective sizes of the layer (of the height of the narrow wall of the waveguide b_{wg} and the thickness of d_c). The parallelepiped of a required volume is obtained by pre-defining the width d_{eff_i} along the axis X , which is calculated by the formula:

$$d_{eff_i} = \frac{\delta_i \cdot d_c}{d_{layer}},$$

where δ_i is a width of a thread part d_c in the studied layer of the width d_{layer} . If $d_c = d_{layer}$, then $d_{eff_i} = \delta_i$.

Each layer can be considered as a material of the matrix with heterogeneities in the waveguide cross section as extended plates of a various thickness. Some layers contain one plate, so do some several ones, while some of them are homogeneous layers of the material of the matrix without inclusions. With a system of coordinates selected

in Fig. 3 and 6, the TE_{10} -type electromagnetic wave has a component of strength of the electric field only along the axis Y . At the same time, a half-wavelength is fit along the axis X (the wide wall of the waveguide). Strength of the electric field is the highest in the middle of the waveguide cross section and decreases closer to the narrow wall. Therefore, a nature of the distribution of threads along the axis X can affect the frequency characteristics of the composite. The distributions of the threads along the axis X in the multi-layer model and the real composite coincide, thereby making it possible to take into account heterogeneity of filling along the axis X . With reduction of the thread thickness, the random distribution along the axis Z in the multi-layer model of the composite is close to the real composite. Thus, it can be expected that the multi-layer model will quite accurately describe interaction of the field with the real material. Attention should be paid that a ratio $\frac{d_{comp}}{d_c}$ that determines the number of the layers is generally is not an integer. Therefore, the thickness of the last layer $d_{last} \leq d_c$. Thus, the multi-layer model of the composite can be represented as follows:

$$\underbrace{S}_{d_{comp}^{comp}} = \underbrace{w_n S_n}_{d_{last}^{\gamma_n^{MPL}}} \underbrace{w_{n-1} U_1^{n-1}}_{d_c^{\gamma_1^{MPL}}}. \quad (8)$$

The constants of propagation γ_i^{MPL} ($i = 1, 2, \dots, n$) are calculated for each layer in the required frequency range.

4.2. Taking into account a distribution of the inclusions along the axis X

When the standard waveguide with the TE_{10} wave is used, twofold orientation of an interface between the media — the layers is possible: when the interfaces are parallel to power lines of the electric field and when they are perpendicular to them. In the first case (Fig. 3, a, b, e), the field in the layers is represented using the TE_{m0} waves, in particular, the TE_{10} waves. When all the boundary conditions are realized for the electric and magnetic components of the electromagnetic wave, a system of consistent equations is obtained to provide a relation between wave numbers, i.e. a dispersion equation. Whence, it is possible to determine the constant of propagation along the axis Z . In this case, one has to calculate high-order determinants.

The constant of propagation of the microwave γ_i^{MPL} can be also determined in each layer of the model using the perturbation theory method as long as the thread thickness satisfies the conditions $d_c \ll (2a_{wg}/\pi)$ and $d_c |\varepsilon_c - 1| \ll (\pi/a_{wg})(2/\omega^2 \varepsilon_0 \mu_0)$ [20]. These conditions define a frequency range of electromagnetic waves, in which use of the model being developed can be applied.

The problem is reduced to calculating the constant of propagation in the waveguide that has heterogeneity in the cross section as plates oriented parallel to the narrow wall of the waveguide (to the axis Y) and extended along the

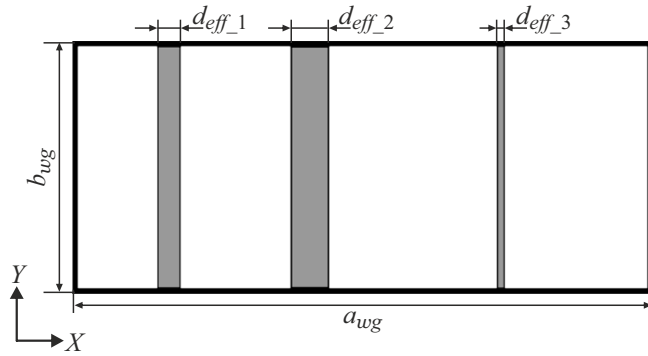


Figure 7. Waveguide cross section containing one of the composite layers.

direction (along the axis Z) of propagation of the microwave (Fig. 7).

A formula of volume perturbation of the waveguide is derived [21] directly from the Maxwell equations and written as follows:

$$\Delta\gamma = \gamma_n - \gamma_0 = \omega \frac{\int_{S_n} (\Delta\varepsilon \cdot E_n \cdot \overline{E_0} + \Delta\mu \cdot H_n \cdot \overline{H_0}) ds}{\int_{S_0} ([\overline{E_0} \times H_n] + [E_n \times \overline{H_0}]) ds}, \quad (9)$$

$$\Delta\varepsilon = \varepsilon_n - \varepsilon_0, \quad \Delta\mu = \mu_n - \mu_0,$$

where S_0 is an area of the waveguide cross section; S_n is an area occupied by the perturbing medium; E_0, H_0 is an electric and a magnetic field of the unperturbed waveguide; E_n, H_n is an electric and a magnetic field in the waveguide with perturbation; ε_0, μ_0 is permittivity and permeability of the unperturbed waveguide; ε_n, μ_n permittivity and permeability of a material acting as perturbation; γ_0 is the constant of propagation in the unperturbed waveguide; γ_n is the constant of propagation in the waveguide with perturbation, an upper bar denotes an operation of complex conjugation.

The numerator is integrated across an inclusion's section S_n , since outside S_n $\Delta\varepsilon = 0$ and $\Delta\mu = 0$ everywhere. The expression (9) is an exact relationship and true for any perturbation if the fields are known E_0, H_0, E_n, H_n .

Practical use of the formula (9) shall be preceded by a problem of determining the fields E_n, H_n . In case when the inclusions considered as perturbation of the medium slightly change the field in the waveguide [20], then it can be assumed that

$$E_n = E_0, \quad H_n = \frac{\gamma_n}{\gamma_0} H_0. \quad (10)$$

Within the framework of the considered problem

$$\gamma_0 = \gamma_m, \quad \gamma_n = \gamma_i^{\text{MPL}},$$

$$\varepsilon_0 = \varepsilon_m, \quad \varepsilon_n = \varepsilon_c,$$

$$\mu_0 = \mu_n = 1,$$

where ε_m and ε_c is complex permittivity of the matrix and the threads, γ_m is the constant of propagation in a

pure matrix without threads, γ_i^{MPL} is a sought constant of propagation in the layer with perturbation.

Solving an inverse problem of determining the complex constant of propagation $\gamma_i^{\text{MPL}} = \gamma_i' + i\gamma_i''$ in one of the layers of the multi-layer model of the composite for the frequency γ is reduced to solving the following equation:

$$(\gamma_i' + i\gamma_i'') - \gamma_m - \omega$$

$$\times \frac{\sum_{k=1}^N \{\Delta\varepsilon \cdot E_m(x_k) \cdot \overline{E_m(x_k)} \cdot d_{\text{eff}_k} \cdot b_{wg}\}}{\sum_{j=1}^M \left\{ \left[\overline{E_m(x_j)} \times \left(\frac{\gamma_i' + i\gamma_i''}{\gamma_m} \cdot H_m(x_j) \right) \right] + \left[E_m(x_j) \times \overline{H_m(x_j)} \right] \right\} \cdot ds} = 0, \quad (11)$$

where N is a number of inclusions, x_k is a coordinate of the inclusion of the number k , d_{eff_k} is an effective width of the inclusion of the number k , b_{wg} is a width of the narrow wall of the waveguide (a height of the inclusion). The denominator is summed over the entire area of the waveguide with a small step ds .

For each layer and frequency, computer numerical methods are used to select values (γ_i', γ_i'') , at which the function (11) takes a minimal value.

In case when the interfaces are perpendicular to the electrical component of the microwave in the waveguide (Fig. 3, *c, d*), a representation of the field as the TE_{m0} waves results in inconsistent equations, thereby indicating an incomplete representation of the field of the propagating wave. It can be explained physically. The constant of propagation of the wave shall depend on properties of all the media that are included in an internal cavity of the waveguide. Therefore, energies shall be exchanged between them, which can not happen when a vector of the electric field of the microwave is perpendicular to the interfaces, since a Umov-Pointing vector turns out to be zero. When the wave propagates, a longitudinal component of the electric field appears, which is absent in any wave of the TE class [22]. Therefore, the perturbation theory method and the MPL model are inapplicable for calculating the threads that are oriented perpendicular to the electrical component of the microwave. The field that has longitudinal components shall be described using a linear combination of TE - and TM -waves.

4.3. Writing the transfer matrix for the model of „many perturbation layers“ (MPL)

The composite pattern (8) is integrated into the photon crystal (3) as a central layer. A final pattern of the photon crystal with a dislocation as the composite represented by

the multi-layer model of n -layers is written as

$$\underbrace{\left(\underbrace{\underbrace{\gamma_{air}}_{\infty} X_6}_{d_1} \underbrace{\underbrace{\gamma_p | \gamma_f}_{d_1} \Pi_5^4}_{d_2} \underbrace{\gamma_p}_{d_1} S_4 \right)_{z_3=z_4-d_1} \left(\underbrace{\underbrace{\gamma_n^{MPL}}_{w_n=z_3} S_n}_{d_{last}} \underbrace{\underbrace{\gamma_i^{MPL}}_{w_{n-1}} U_1^{n-1}}_{d_c} \right)_{d_{comp}}}_{z_3=z_4-d_1} \left(\underbrace{\underbrace{\gamma_p}_{z_3-d_{comp}} S_2}_{d_1} \underbrace{\underbrace{\gamma_f | \gamma_p}_{z_1} \Pi_1^4}_{d_2 | d_1} \underbrace{\underbrace{\gamma_{air}}_{z_0=0} X_0}_{\infty} \right) < . \quad (12)$$

Writing the periodic groups Π in detail, we obtain

$$\underbrace{\left(\underbrace{\underbrace{\gamma_{air}}_{\infty} X_{12}}_{d_1} \underbrace{\underbrace{\gamma_p}_{z_{11}} S_{11}}_{d_1} \underbrace{\underbrace{\gamma_f}_{z_{10}} S_{10}}_{d_2} \underbrace{\underbrace{\gamma_p}_{z_9} S_9}_{d_1} \underbrace{\underbrace{\gamma_f}_{z_8} S_8}_{d_2} \underbrace{\underbrace{\gamma_p}_{z_7} S_7}_{d_1} \right)_{z_6=z_7-d_1} \left(\underbrace{\underbrace{\gamma_n^{MPL}}_{w_n=z_6} S_n}_{d_{last}} \underbrace{\underbrace{\gamma_i^{MPL}}_{w_{n-1}} U_1^{n-1}}_{d_c} \right)_{d_{comp}} \left(\underbrace{\underbrace{\gamma_p}_{z_5} S_5}_{d_1} \underbrace{\underbrace{\gamma_f}_{z_4} S_4}_{d_2} \underbrace{\underbrace{\gamma_p}_{z_3} S_3}_{d_1} \underbrace{\underbrace{\gamma_f}_{z_2} S_2}_{d_2} \right)_{z_6=z_7-d_1} \left(\underbrace{\underbrace{\gamma_p}_{z_1} S_1}_{d_1} \underbrace{\underbrace{\gamma_{air}}_{z_0=0} X_0}_{\infty} \right) < . \quad (13)$$

An associativity property of a matrix product makes it possible to separately calculate the transfer matrix \mathbf{T}_{MPL} via the multi-layer model of the composite and include it into a product that calculates the transfer matrix \mathbf{T}_{total} throughout the entire photon crystal:

$$\mathbf{T}_{total} = \mathbf{T}_{left} \cdot \mathbf{T}_{lb} \cdot \mathbf{T}_{MPL} \cdot \mathbf{T}_{rb} \cdot \mathbf{T}_{right}. \quad (14)$$

The matrices \mathbf{T}_{lb} and \mathbf{T}_{rb} are the transfer matrices through the left and right boundaries of the composite represented by the multi-layer MPL model (8) with the left \mathbf{T}_{left} and right \mathbf{T}_{right} parts of the photon crystal. It should be taken into account that coordinates of the layers in all the matrices are counted in one system of coordinates, which is common for the entire photon crystal.

The transfer matrix through the central layer of the pattern (13), which is a dislocation as the multi-layer MPL model of the composite, is written as

$$\begin{aligned} \mathbf{T}_{MPL} &= T(w_{n-1}, \gamma_n^{MPL}, \gamma_{n-1}^{MPL}) \\ &\times T(w_{n-1} - d_c, \gamma_{n-1}^{MPL}, \gamma_{n-2}^{MPL}) \cdot \dots \\ &\times T(w_2 - d_c, \gamma_2^{MPL}, \gamma_1^{MPL}), \end{aligned} \quad (15)$$

where γ_i^{MPL} are constants of propagation in each layer of the multi-layer model, which are found using the perturbation theory from the equation (11), $w_{n-1} = z_6 - d_{last}$.

Substituting the matrix \mathbf{T}_{MPL} (15) into the expression (14) results in the following kind of the final transfer matrix through the photon crystal with a dislocation as the multi-layer structure:

$$\begin{aligned} \mathbf{T}_{total} &= \mathbf{T}^{(11)}(z_{11}, \gamma_{air}, \gamma_p) \cdot \mathbf{T}^{(10)}(z_{11} - d_1, \gamma_p, \gamma_f) \\ &\times \mathbf{T}^{(9)}(z_{10} - d_2, \gamma_f, \gamma_p) \cdot \mathbf{T}^{(8)}(z_9 - d_1, \gamma_p, \gamma_f) \\ &\times \mathbf{T}^{(7)}(z_8 - d_2, \gamma_f, \gamma_p) \cdot \mathbf{T}^{(6)}(z_7 - d_1, \gamma_p, \gamma_n^{MPL}) \\ &\times \mathbf{T}_{MPL} \cdot \mathbf{T}^{(5)}(z_6 - d_{comp}, \gamma_1^{MPL}, \gamma_p) \\ &\times \mathbf{T}^{(4)}(z_5 - d_1, \gamma_p, \gamma_f) \cdot \mathbf{T}^{(3)}(z_4 - d_2, \gamma_f, \gamma_p) \\ &\times \mathbf{T}^{(2)}(z_3 - d_1, \gamma_p, \gamma_f) \cdot \mathbf{T}^{(1)}(z_2 - d_2, \gamma_f, \gamma_p) \\ &\times \mathbf{T}^{(0)}(z_1 - d_1, \gamma_p, \gamma_{air}), \end{aligned} \quad (16)$$

where

$$\begin{aligned} \mathbf{T}_{left} &= \mathbf{T}^{(11)}(z_{11}, \gamma_{air}, \gamma_p) \cdot \mathbf{T}^{(10)}(z_{11} - d_1, \gamma_p, \gamma_f) \\ &\times \mathbf{T}^{(9)}(z_{10} - d_2, \gamma_f, \gamma_p) \cdot \mathbf{T}^{(8)}(z_9 - d_1, \gamma_p, \gamma_f) \\ &\times \mathbf{T}^{(7)}(z_8 - d_2, \gamma_f, \gamma_p), \\ \mathbf{T}_{right} &= \mathbf{T}^{(4)}(z_5 - d_1, \gamma_p, \gamma_f) \cdot \mathbf{T}^{(3)}(z_4 - d_2, \gamma_f, \gamma_p) \\ &\times \mathbf{T}^{(2)}(z_3 - d_1, \gamma_p, \gamma_f) \cdot \mathbf{T}^{(1)}(z_2 - d_2, \gamma_f, \gamma_p) \\ &\times \mathbf{T}^{(0)}(z_1 - d_1, \gamma_p, \gamma_{air}), \\ \mathbf{T}_{lb} &= \mathbf{T}^{(6)}(z_7 - d_1, \gamma_p, \gamma_n^{MPL}), \\ \mathbf{T}_{rb} &= \mathbf{T}^{(5)}(z_6 - d_{comp}, \gamma_1^{MPL}, \gamma_p). \end{aligned}$$

By substituting (16) into (6), we calculate the spectrum of the reflection coefficient $R_{MPL}(\omega)$ of the photon crystal with a dislocation as the composite that is represented by many „perturbation layers“ (MPL).

5. Lamellar model of the composite (EPM)

A simpler model is a replacement of the threads with equally-thick plates that are equidistantly arranged along the wide wall of the waveguide and extended along the direction of propagation of the microwave (Fig. 8). We call it the Equidistant Plates Model (EPM).

A thickness of the plates d_{pl} and a distance between them L_{pl} are calculated by the formulas

$$d_{pl} = (v_c \times a_{wg}) / N_{pl},$$

$$L_{pl} = a_{wg} / (N_{pl} + 1),$$

where v_c is a volume portion of the inclusions in the composite, a_{wg} is a size of the wall of the waveguide, relative to which the plates are perpendicular, N_{pl} is a number of the plates.

Table 2. List of the studied models

Designation	Description	Calculation procedure
FEM	Finite Elements Method. Uniform volume distribution of threads oriented along the electrical component of the microwave (parallel to the narrow wall of the waveguide). Finite element method using the HFSS software	
MPL	Many Perturbation Layers. Multi-layer model, the inclusions are threads with an effective width along the axis X . Perturbation theory, in the Mathcad software package.	
EPM	Equidistant Plates Model. „Lamellar model“, thin extended plates.	
EMT	Effective Medium Theory. Maxwell-Garnett theory of effective permittivity. The threads are replaced by elongated ellipses [23].	Calculation by the formula (18)

We will investigate a deviation of parameters calculated using the models MPL, EPL, EMT, from parameters determined when simulating by the finite element method (FEM). A deviation measure will be assumed to be a relative magnitude

$$\delta X^k = \sqrt{\frac{(X^k - X^{\text{FEM}})^2}{X^{\text{FEM}}}} \cdot 100\%, \quad (21)$$

where X is a considered parameter, $k = \text{MPL, EPL, EMT}$ is a model for which the deviation of the parameter X is calculated. The parameter X in (21) may be a frequency f_{\min} or a magnitude R_{\min} of the reflection coefficient minimum, permittivity ϵ_{comp} or electrical conductance σ_{comp} of the composite.

7.1. Applicability of the model of many „perturbation layers“ (MPL) for calculating the spectrum of the reflection coefficient

The spectra of the microwave reflection coefficient of the photon crystal with the dislocation as the composite (Fig. 3, *a*), which are calculated using the models FEM and MPL at the small volume portions, coincide with each other (Fig. 9).

With an increase of the number of the threads N_c , a frequency dependence of the reflection coefficient, which is calculated using the models of many „perturbation layers“ (MPL), correlates with results of the calculation according to the FEM model (Fig. 10). Since the two different calculation methods result in the same result, it can be concluded that it is justifiable to use the results of HFSS simulation as reference ones. The width of the threads with their small number and the large volume portion increases. As a result, accuracy of an approximation (10) used in the perturbation theory decreases and there is an increase of a divergence of results obtained using the model of many „perturbation layers“ (MPL) with results obtained by the finite element method (FEM).

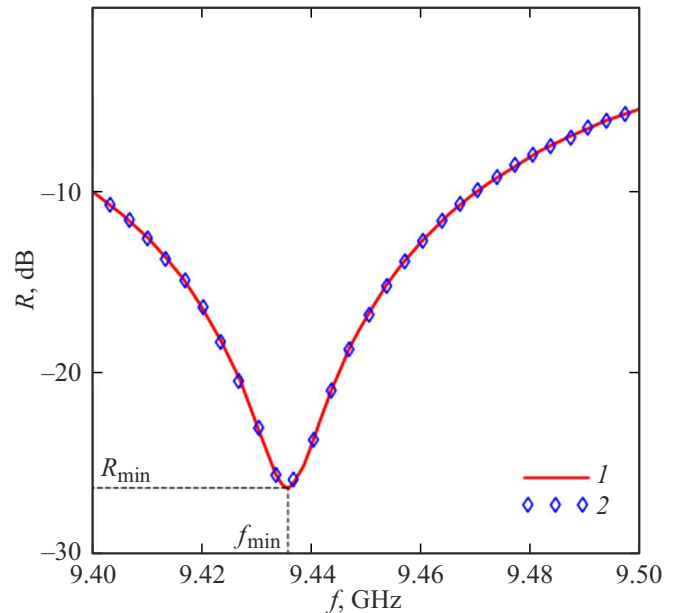


Figure 9. Spectrum of the reflection coefficient of the photon structure, which is calculated using: 1 — the FEM method, 2 — the MPL model. The dislocation is provided by the composite with the following parameters: $N_c = 1.6 \text{ pcs/mm}^2$, $\nu_c = 0.5\%$, $\epsilon_c = 50$, $\sigma_c = 5 \Omega^{-1} \text{ m}^{-1}$.

The frequency f_{\min} (Fig. 10, *a*) and the magnitude R_{\min} (Fig. 10, *b*) of the reflection coefficient minimum oscillate due to the random distribution of threads. These oscillations can not be described by the effective medium models. Therefore, it is proposed to increased accuracy of calculation of the electrophysical parameters of the structures containing the oriented threads using the model being developed.

When the number of the threads exceeds 1.5 pcs/mm^2 , the deviation of the frequency of the reflection coefficient

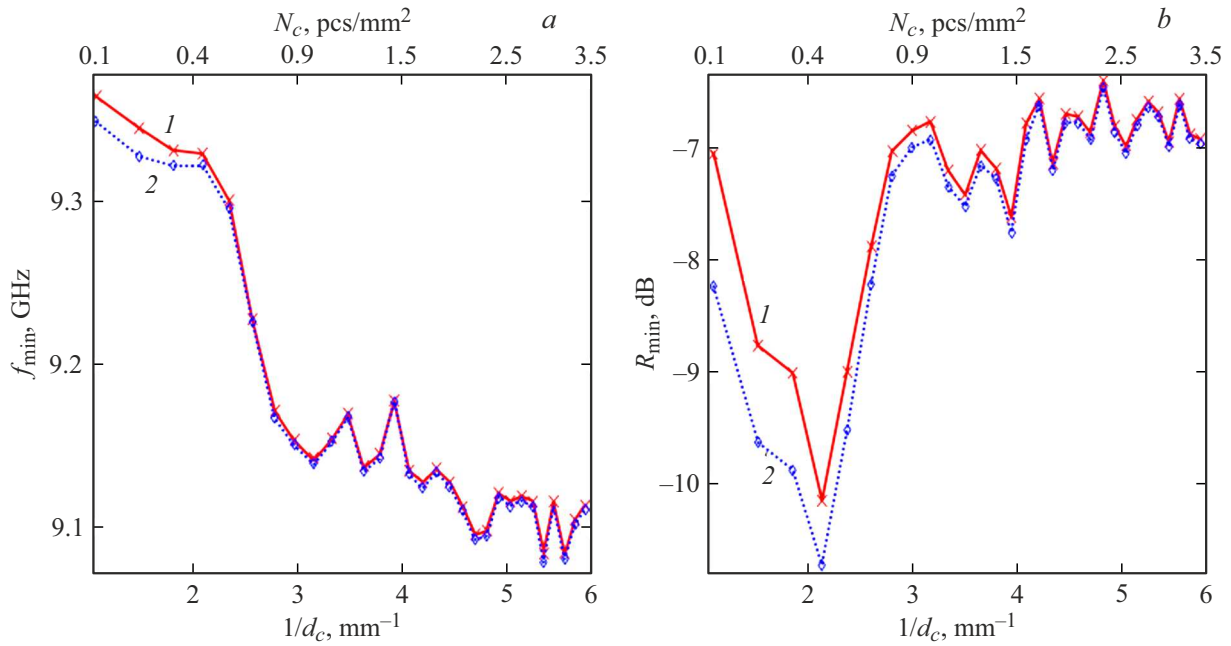


Figure 10. Dependence of the frequency f_{\min} (a) and the magnitude R_{\min} (b) of the reflection coefficient minimum on a reciprocal thickness of the threads (the respective number of the threads is specified above), it was calculated using: 1 — the finite element method (FEM), 2 — the model of many „perturbation layers“ (MPL). The volume portion of the threads in the composite $v_c = 10\%$.

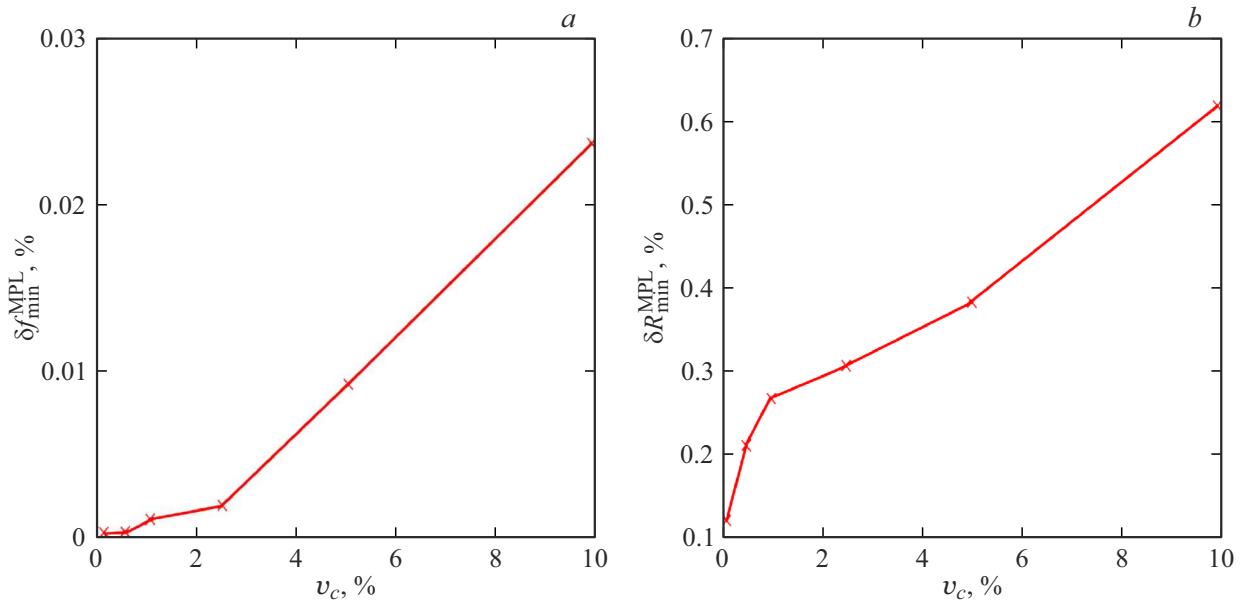


Figure 11. Deviation of the frequency $\delta f_{\min}^{\text{MPL}}$ (a) and the magnitude $\delta R_{\min}^{\text{MPL}}$ (b) of the reflection coefficient minimum of the volume portion of inclusions when the number of the threads $N_c = 1.6 \text{ pcs/mm}^2$.

minimum does not exceed 0.05% (Fig. 11, a), while the deviation of the magnitude of the minimum does not exceed 1% (Fig. 11, b).

Let us consider the influence of the parameters of inclusions ϵ_c and σ_c on accuracy of the calculations using the MPL model at the various volume portions of inclusions v_c . The studied composites are selected to be samples with the number of the threads $N_c = 1.6 \text{ pcs/mm}^2$, at which an error caused by the sizes of the threads is insignificant.

The dependence of the deviation of the frequency $\delta f_{\min}^{\text{MPL}}$ and the magnitude $\delta R_{\min}^{\text{MPL}}$ of the reflection coefficient minimum on a real part of permittivity and electrical conductance of inclusion is shown in Fig. 12.

The model of many „perturbation layers“ (MPL) when the volume portions of inclusions $v_c < 2.5\%$ is a good approximation for calculating the reflection coefficient of the composites when the parameters of inclusions $\epsilon_c < 100$, $\sigma_c < 100$. The error of determining the reflection coefficient minimum is $\delta f_{\min}^{\text{MPL}} < 0.2\%$, $\delta R_{\min}^{\text{MPL}} < 1.0\%$.

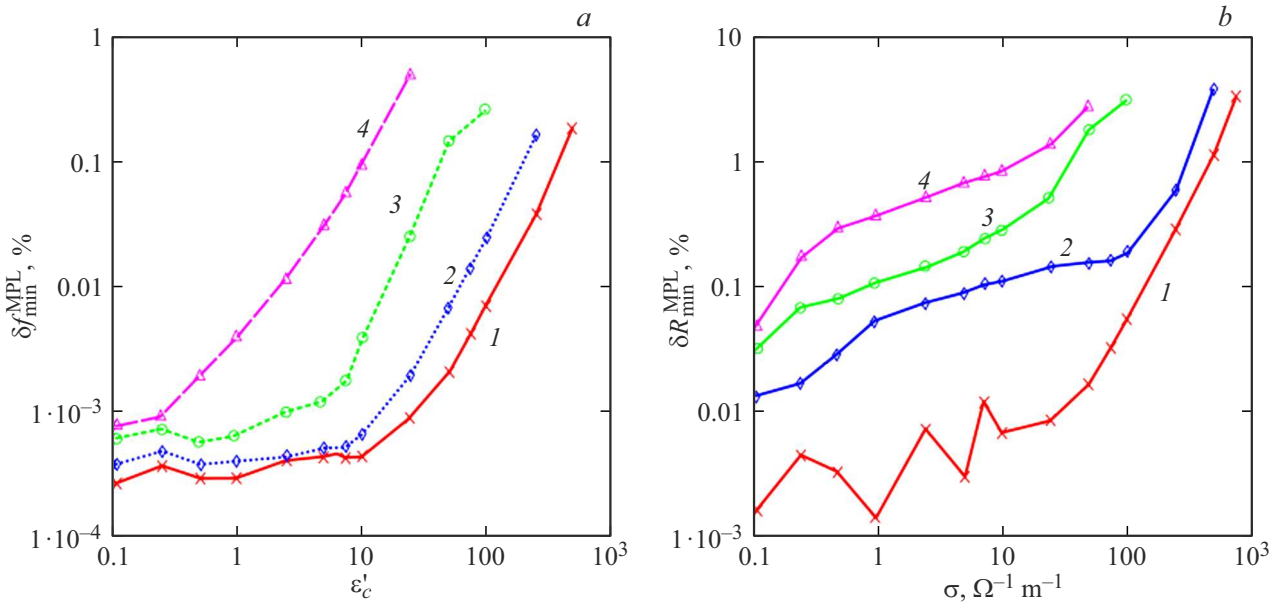


Figure 12. Dependence of the deviation of the frequency of the minimum $\delta f_{\min}^{\text{MPL}}$ on permittivity of inclusions ϵ_c (a) and the magnitude of the minimum $\delta R_{\min}^{\text{MPL}}$ on conductivity of inclusions σ_c (b) when the number of the threads $N_c = 1.6 \text{ pcs/mm}^2$ and with the volume portions of inclusions ν_c : 1 — 0.5%, 2 — 1.0%, 3 — 5.0%, 4 — 10.0%.

The increase of the volume portion of the threads ν_c results in an increase of the error. However, with the small values of permittivity and conductivity of the threads ($\epsilon_c < 40$, $\sigma_c < 10$) the calculations made using the model of „perturbation layers“ (MPL) result in an error of determining the reflection coefficient minimum, which does not exceed 1% even at the large volume portions of inclusions $\nu_c = 10\%$.

With an increase of electrical conductance of inclusions σ_c the Q factor of the structure decreases and resonance on the frequency dependence is less pronounced. Correspondingly, it is expected that accuracy of determining the parameters by the experimental spectra will decrease when values of electrical conductance σ_c are high. Applicability of the MPL model can be estimated by Fig. 13, in which for each volume portion of inclusions their electrical conductance σ_{c50} is represented, at which the resonance Q factor decreases in 50 times relative to the pure matrix without inclusions (the magnitude of the reflection coefficient minimum increases from -40 to -4 dB). At the same time, the error of determining complex permittivity of the composite will not exceed 1%.

7.2. Determining the electrophysical parameters of homogeneous composites using the lamellar EPM model

The calculation by the MPL model requires data about the exact spatial distribution of inclusions, which can be difficult to obtain, while the EPM model requires to know only a number of the plates.

We investigate usability of the lamellar EPM model for determining the parameters of the composites containing the equispaced threads. Let us consider the composite that is a matrix of epoxy resin with the following parameters of the threads: $\nu_c = 0.5\%$, $\epsilon_c = 50$, $\sigma_c = 5 \Omega^{-1} \text{m}^{-1}$. An inverse problem of determining the electrophysical parameters of the composite is solved based on data about the frequency and value of the reflection coefficient minimum of the photon structure. The dependence of these magnitudes on the number of the threads is shown in Fig. 13.

Stochastic oscillations of the frequency f_{\min} (Fig. 14, a, the curve 1) and the magnitude R_{\min} (Fig. 14, b, the curve 1) of the reflection coefficient minimum, which are obtained as a result of HFSS simulation, tend to a value calculated by the lamellar EPM model when the number of the threads exceeds two hundred ($N_c > 2 \text{ pcs/mm}^2$). The dependences of the frequency and the magnitude of the reflection coefficient minimum, which are calculated by the lamellar EPM model (Fig. 14, the curves 2), achieve saturation when the number of the plates exceeds several tens.

The real part of effective permittivity of the composite and its effective electrical conductance were determined as a result of solving the inverse problem (20). The dependences of a value of the calculated parameters on the number of the threads are shown in Fig. 15, a, b. The error of determining the parameters (21) of the composite, which are found by the spectrum calculated using the lamellar EPM model, is shown in Fig. 15, c, d.

Thus, the error of determining the electrophysical parameters of the homogeneous composite depends on the random distribution of the threads, which is difficult to

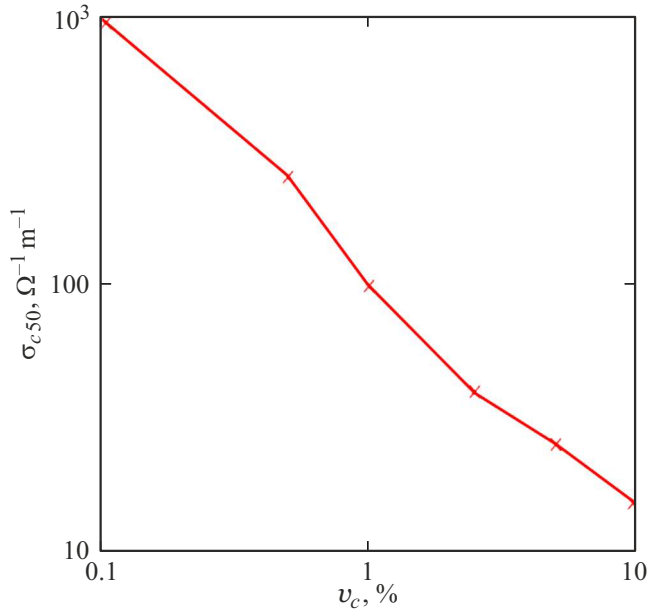


Figure 13. Dependence of electrical conductance, at which the resonance Q factor decreases in 50 times relative to the pure matrix, on the volume portion of inclusions.

be experimentally determined. The „lamellar model“ makes it possible to calculate the real part of permittivity with a model imperfection error of at most 1% and electrical conductance with the same of at most 10% (when the volume portion of inclusions $v_c = 1\%$ and their number $N_c > 1.0 \text{ pcs/mm}^2$).

The EPM model made it possible to determine the parameters of the filamentary inclusions of the real composite, which are oriented along the axis Y , which was dried in presence of the magnetic field with induction of 130 mT. Effective complex permittivity of the composite $\epsilon_{comp\parallel}$ was calculated using the experimentally-measured spectrum of the reflection coefficient (Fig. 2, a, the curve 2). The found value was used when solving the inverse problem (Fig. 16) for determining complex permittivity $\epsilon_{c\parallel}^{EPM}$ of the CNT inclusions using the lamellar EPM model (Fig. 3, b) (Table 3). The error of determining the parameters relative to the values of $\epsilon_{c\parallel}^{FEM}$, which are calculated by the FEM model (Fig. 3, a), was $\delta\epsilon_c^{EPM} = 4\%$ and $\delta\sigma_c^{EPM} = 6\%$.

The „lamellar model“ is inapplicable in case of perpendicular orientation of the plates (Fig. 3, d) relative to the electric component of the microwave (Fig. 17). As known [26], it is possible to find in the waveguide excited to any of the wave types planes that are in all points normal to electric power lines and tangent to magnetic power lines. A field of this wave will not be excited if the waveguide includes thin ideally conductive surface that coincide with these planes. As a result, the rectangular waveguide excited to the TE_{10} -type wave can be divided into any arbitrarily large number of waveguides with an invariable size a_{wg} and a reduced size b_{wg} . Judging by the fact that the value of the frequency

Table 3. Values of the electrophysical parameters of the composites and the filamentary inclusions, which are determined by the experimental data

ϵ	ϵ'	ϵ''	$\sigma, \Omega^{-1} m^{-1}$	Figure
ϵ_{comp}	3.23	0.03	0.01	Fig. 2, a, the curve 1
$\epsilon_{comp\parallel}$	3.51	0.09	0.05	Fig. 2, a, the curve 2
$\epsilon_{c\parallel}^{FEM}$	55.20	11.48	6.04	Fig. 3, a
$\epsilon_{c\parallel}^{EPM}$	53.0	12.11	6.4	Fig. 3, b

and the magnitude of the minimum (Fig. 17, the curve 2) is slightly affected by presence of the plates, one can say that in case of the lamellar model the electromagnetic field weakly interacts with the perpendicular-oriented plates. As a result, the reflection coefficient minimum is slightly different from the pure matrix without inclusions.

7.3. Comparison of values of the parameters, which are calculating using the various models

The effective medium model (EMT) is applied for calculating complex permittivity of homogeneous media. As shown above, the dependence of the reflection coefficient minimum on the number of inclusions exhibits the stochastic oscillations, which tend to a certain average value with an increase of the number of inclusions. An increase of the number of the threads results in a significant increase of the time of calculation by the finite element method (FEM) when the number of the threads $N_c > 5.0 \text{ pcs/mm}^2$ and their thickness $d_c < 15 \mu\text{m}$. When the volume portions are small or the values of permittivity and conductivity of inclusions are low, the finite element method (FEM) can be replaced by calculation using the model of many „perturbation layers“ (MPL).

An error of determining the parameters of the homogeneous composite using the model of many „perturbation layers“ (MPL) will be estimated by a formula of Mean Relation Percentage Error (MRPE):

$$\delta X_{avg}^{MPL}(v_c) = \frac{1}{n} \sum_{i=0}^{n-1} \frac{\sqrt{\left(X_{MPL}(N_i, v_c) - \frac{\sum_{i=0}^{n-1} X_{MPL}(N_i, v_c)}{n} \right)^2}}{X_{MPL}(N_i, v_c)}, \quad (22)$$

where X_{MPL} is a parameter (ϵ' or σ), whose error is calculated, which is calculated using the MPL model with the volume portion of the threads v_c and their number N_i , n is a number of the composites, which are averaged.

The error of determining the parameters using the lamellar EPM model or by the effective medium method (EMT) will be estimated using an error of the parameter found by the MPL method, which is relative to the average value, since the MPL model well correlates with the FEM

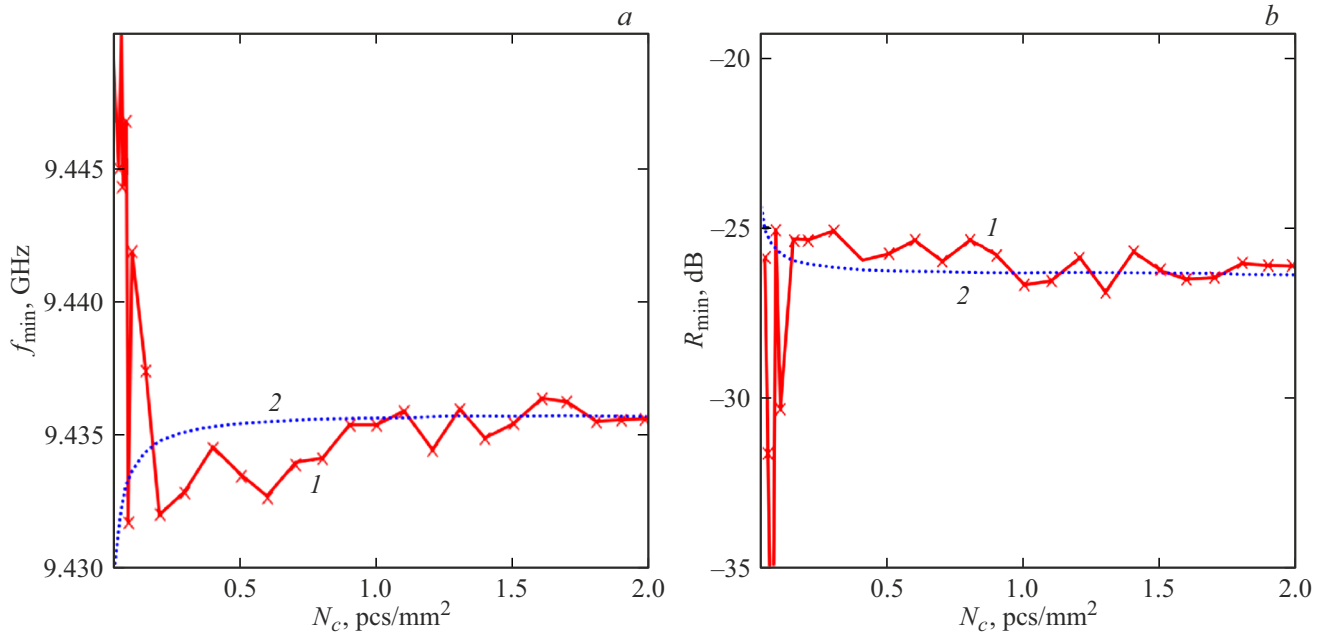


Figure 14. Dependence of the frequency (a) and the magnitude (b) of the reflection coefficient minimum of the photon structure with the dislocated layer as the sample of the studied composite ($v_c = 0.5\%$, $\varepsilon_c = 50$, $\sigma_c = 5 \Omega^{-1}\text{m}^{-1}$) on the number of inclusions N_c , the calculations were performed using: 1 — the finite element method (FEM), 2 — the perturbation theory for the lamellar EPM model.

method:

$$\delta X_{avg}^{\text{EPM}}(v_c) = \frac{X_{\text{EPM}}^{\text{EPM}}(N_i, v_c) - \frac{\sum_{i=0}^{n-1} X_{\text{MPL}}(N_i, v_c)}{n}}{\frac{\sum_{i=0}^{n-1} X_{\text{MPL}}(N_i, v_c)}{n}}. \quad (23)$$

The dependence $\delta\varepsilon_{avg}$ and $\delta\sigma_{avg}$ on the volume portion of inclusions is shown in Fig. 18 and Table 4. When calculating the errors by the formulas (22) and (23), the number of the threads in the composites N_i varied from 1000 to 1500 with the step of 50, i.e. $n = 10$.

A slight decrease of the average relative error (Fig. 18, the curve 1) with an increase of the volume portion of the threads is due to reduction of stochastic oscillations of the frequency and the magnitude of the reflection coefficient minimum, which is related to the more uniform distribution of the threads when the large portions are large.

When the volume portions are small $v_c < 1\%$, the effective medium model (EMT) and the „lamellar EPM model“ describe the real part of permittivity of the composite with high accuracy, but result in the increased values when determining electrical conductance. This strange kind (Fig. 18, b, the curves 2, 3) of the dependence of the error can be explained by stochastic oscillations (Fig. 10) and a calculated value of the error will depend on selecting a range of the number of the threads, which was used when calculating a summand $\frac{\sum_{i=0}^{n-1} X_{\text{MPL}}(N_i, v_c)}{n}$ in (23). When the volume portions are small, the selected range (from 1000 to 1500 threads) results in decreased values of electrical conductance relative to the value calculated by the EMT method and in the increased ones when they are high. It

Table 4. Error of determining the electrophysical parameters using the various models (the parameters of the threads $\varepsilon_c = 50$, $\sigma_c = 5 \Omega^{-1}\text{m}^{-1}$)

v_c	Error, %					
	$\delta\varepsilon_{avg}^{\text{MPL}}$	$\delta\varepsilon_{avg}^{\text{EPM}}$	$\delta\varepsilon_{avg}^{\text{EMT}}$	$\delta\sigma_{avg}^{\text{MPL}}$	$\delta\sigma_{avg}^{\text{EPM}}$	$\delta\sigma_{avg}^{\text{EMT}}$
0.5 %	0.09	+0.27	+0.3	0.01	+2.60	+3.76
2.5 %	0.09	-1.15	-0.93	0.63	-2.41	-0.91
5 %	0.55	-2.51	-2.02	1.32	-3.30	-1.57
10 %	0.51	-5.87	-4.67	1.05	-4.78	-2.71

may indicate existence of a dependence of values of the parameters of the composite on the number of the threads per a unit area with a fixed volume portion, which requires separate research.

Thus, with the increase of the volume portion of inclusions there is an increase of divergence of the values of permittivity and electrical conductance of the composites, which are determined using the MPL model, from the values calculating using the lamellar EPM model and the effective medium model (EMT).

7.4. Calculation of the reflection coefficient of the heterogeneous composite

Unlike the effective medium model, the MPL model is applicable for calculating the reflection coefficient of the

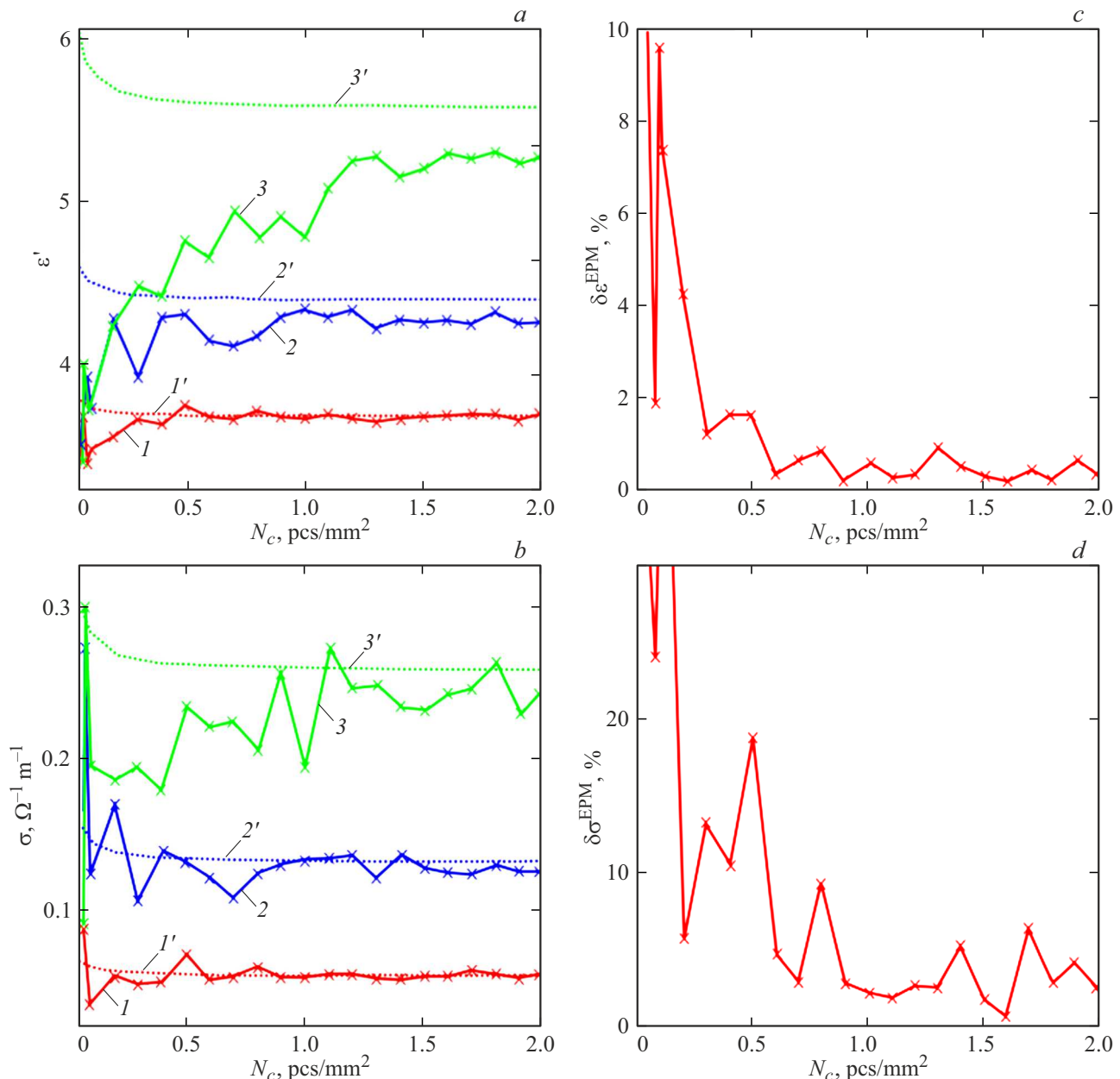


Figure 15. Dependence of the real part of effective permittivity ε' (a) and electrical conductance σ (b) of the composite on the number of inclusions, which is calculated using the FEM model (the curves 1–3) and the EPM model (the curves 1'–3') when the volume portions of inclusions v_c are: 1 — 1%, 2 — 2.5%, 3 — 5%; a deviation of the values of effective permittivity (c) and electrical conductance (d) of the composite, which are calculated by the EMP model, from the FEM model when the volume portion of inclusions $v_c = 1\%$.

heterogeneous composites (Fig. 3, e). It is exemplified by a considered composite, in which the inclusions are shifted from the narrow walls of the waveguide to a middle of the wide wall (Fig. 19, a). The following designations are used in Fig. 19: V_0 is a total volume of the composite, V_A is a central portion of the waveguide, in which the threads are distributed, R_A is a reflection coefficient minimum with heterogeneous filling (the threads are distributed across the volume V_A), R_0 is the same with homogeneous filling ($V_A = V_0$).

The closer the threads to the middle, the higher the reflection coefficient minimum (Fig. 19, b), which is due to distribution of the electric field in the waveguide, which takes a maximum value in the middle of the wide wall. Thereby, the MPL model explains an increase of the minimum of the microwave reflection coefficient (Fig. 2, b) of the ER-ML-CNT composites, which is experimentally observed and related to contraction of the ML and CNT suspension closer to the sample center when the composite is dried when applying the heterogeneous magnetic field.

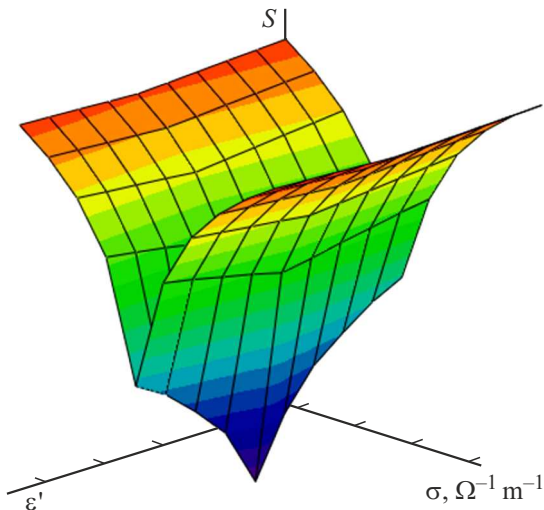


Figure 16. Minimum of a residual function when solving the inverse problem of determining the parameters of inclusions; the frequency dependence of the reflection coefficient of the composite was calculated using the lamellar EPM model.

Conclusion

Thus, we have proposed a model that makes it possible to reduce a portion of the waveguide filled with a dielectric with oriented inclusions to the multi-layer structure, i.e. „the model of many perturbation“ layers (MPL). The reflection coefficient of this structure can be calculated using the transfer matrix method, wherein the constant of propagation

of each layer is calculated using the perturbation theory. The spectra obtained using the MPL model agree with results of HFSS simulation by the finite element method. The error of determining the reflection coefficient minimum does not exceed 1% when the volume portions are small or values of complex permittivity of inclusions are low. The MPL model is suitable for calculating structures with a large number of micron-size threads, whereas other simulation methods require time consumption by at least an order when the thickness of the threads is below $15\ \mu\text{m}$.

The electrophysical parameters of the composite were calculated by a position of the microwave reflection coefficient minimum of the photon structure with the dislocation as the studied sample when solving the inverse problem. At the same time, the error of determining the parameters of the composite does not exceed 1%. It is expedient to use the photon structure when the volume portions are small or the values of electrical conductance of inclusions are low, since the resonance Q factor decreases when the values are high. For example, when $\sigma_c = 25\ \Omega^{-1}\text{m}^{-1}$ and $v_c = 10\%$ the error of determining electrical conductance is 2.4%, and when $\sigma_c = 50\ \Omega^{-1}\text{m}^{-1}$ it is already 8.3%.

When the volume portions are high ($v_c > 5\%$), the numerical calculation done using the model of many perturbation layers (MPL) results in an error of determining complex permittivity that is in five times less than when using the Maxwell-Garnett effective medium method (EMT) in an approximation of extended ellipsoids.

We have also considered applicability of the model of many perturbation layers (MPL) for calculating the spectrum of the reflection coefficient of the composites

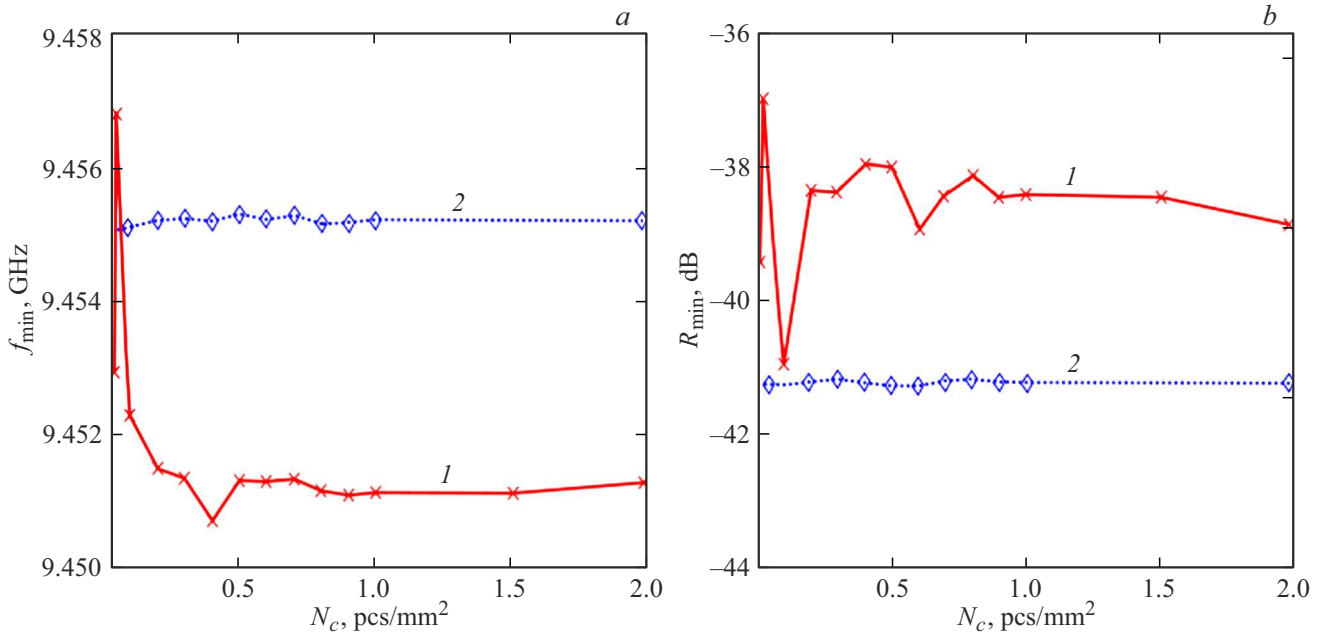


Figure 17. Dependence of the frequency f_{\min} (a) and the magnitude R_{\min} (b) of the reflection coefficient minimum on the number of the threads (the curve 1) and the plates (the curve 2), which are oriented perpendicular to the electrical component of the microwave (parallel to the wide wall of the waveguide). It was calculated by the finite element method (FEM).

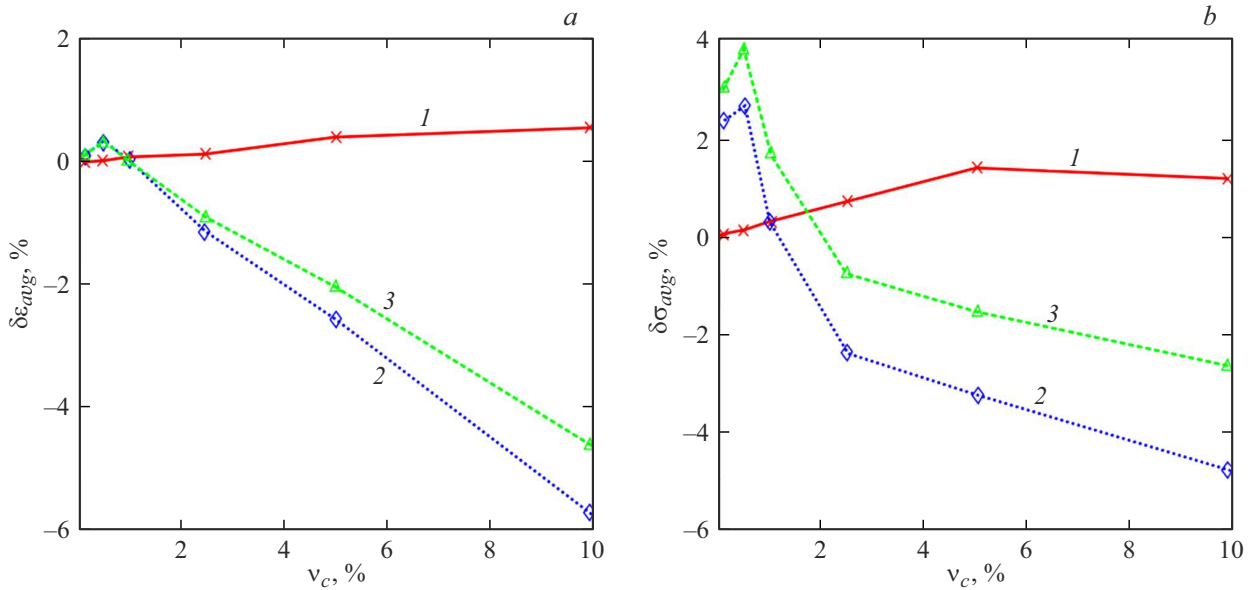


Figure 18. Dependence of the error of determining the real part of permittivity (a) and electrical conductance (b) of the composite with uniformly distributed inclusions on the volume portion of inclusions with the parameters $\varepsilon_c = 50$, $\sigma_c = 5 \Omega^{-1} \text{m}^{-1}$: 1 — an average relative error during calculations when using the MPL model, 2 is a relative deviation of the values of the parameters, which are calculated using the MPL model, from the EMP model, 3 — from the EMT model.

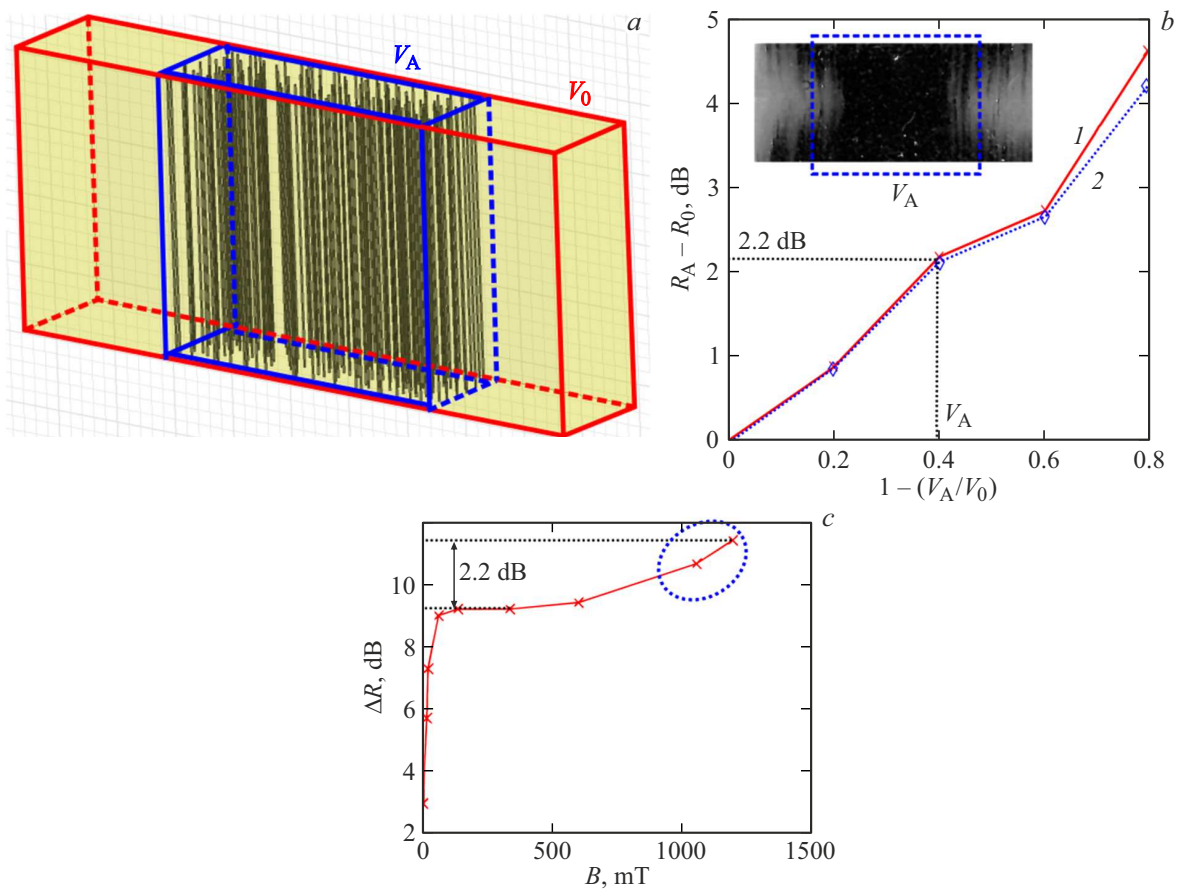


Figure 19. Heterogeneous filling of the waveguide (a), a difference of the reflection coefficient minima between heterogeneous and homogeneous filling on a reduced volume (b) (the insert includes a photo of the sample) and an experimental dependence of the difference of the reflection coefficient minima ΔR of the samples dried in presence of/without the magnetic field on the value of induction of the magnetic field (c). The spectrum was calculated: 1 — in HFSS, 2 — using the model of many „perturbation layers“ (MPL).

with a heterogeneous distribution of the oriented threads. The results well agree with the data obtained during HFSS simulation.

Conflict of interest

The authors declare that they have no conflict of interest.

References

- [1] H. Shanmugasundram, E. Jayamani, K. Soon. *Renewable Sustainable Energy Rev.*, **157** (3), 112075 (2022). DOI: 10.1016/j.rser.2022.112075
- [2] L. Zhao, C. Wei, Z. Li, W. Wei, L. Jia, X. Huang, W. Ning, Z. Wang. *J. Ren. Mater. Design*, **210** (16), 110124 (2021). DOI: 10.1016/j.matdes.2021.110124
- [3] L. Cui, X. Han, F. Wang, H. Zhao, Y. Du. *J. Mater. Sci.*, **56**, 10782 (2021). DOI: 10.1007/s10853-021-05941-y
- [4] R. Li, X. Yang, J. Li, Y. Shen, L. Zhang, R. Lu, C. Wang, X. Zheng, H. Chen, T. Zhang. *Mater. Today Phys.*, **22**, 100594 (2022). DOI: 10.1016/j.mtphys.2021.100594
- [5] L. Li, J. Cheng, Y. Cheng, T. Han, Y. Liu, Y. Zhou, Z. Han, G. Zhao, Y. Zhao, C. Xiong, L. Dong, Q. Wang. *J. Mater. Chem.*, **9**, 23028 (2021). DOI: 10.1039/D1TA05408B
- [6] V.E. Ogbonna, A.P.I. Popoola, O.M. Popoola. *Polymer Bull.*, **80**, 3449 (2023). DOI: 10.1007/s00289-022-04249-4
- [7] E.A. Vorob'eva, A.P. Evseev, V.L. Petrov, A.A. Shemukhin, N.G. Chechenin. *VMU. Seriya 3. Fizika. Astronomiya*, **1**, 23 (2021) (in Russian).
- [8] L.A. Apresyan, D.V. Vlasov, D.A. Zadorin, V.I. Krasovskii. *Tech. Phys.*, **62** (1), 6 (2017). DOI: 10.1134/S1063784217010029
- [9] H. Looyenga. *Physica*, **31**, 401 (1965). DOI: 10.1016/0031-8914(65)90045-5
- [10] S.O. Nelson. *Transactions ASAE*, **35** (2), 625 (1992). DOI: 10.13031/2013.28642
- [11] G.S. Kats, D.V. Milevski. *Napolniteli dlya polimernykh kompozitsionnykh materialov* (Khimiya, M., 1981) (in Russian).
- [12] A.N. Lagarkov, S.M. Matytsin, K.N. Rozanov, A.K. Sarychev. *J. Appl. Phys.*, **84** (7), 3806 (1998). DOI: 10.1063/1.368559
- [13] X. Xu, A. Qing, Y.B. Gan, Y.P. Feng. *J. Electromagn. Waves Appl.*, **18** (5), 649 (2004). DOI: 10.1163/156939304774114682
- [14] D.W. Seo, H.J. Kim, K.U. Bae, N.H. Myung. *J. Electromagnetic Waves Applications*, **24** (17–18), 2419 (2010). DOI: 10.1163/156939310793675835
- [15] M.J. Akhtar, H.B. Baskey, P. Ghising, N.M. Krishna. *IEEE Transactions on Dielectrics and Electrical Insulation*, **22** (3), 1702 (2015). DOI: 10.1109/TDEL.2014.004808
- [16] A.E. Postel'ga, S.V. Igonin. *Defektoskopiya*, **2**, 53 (2025) (in Russian).
- [17] D.A. Usanov, M.K. Merdanov, A.V. Skripal', D.V. Ponomarev. *Izvestiya Sar. un-ta. Novaya seriya. Seriya: Fizika*, **15** (1), 57 (2015) (in Russian). DOI: 10.18500/1817-3020-2015-15-1-57-73
- [18] D.A. Usanov, S.A. Nikitov, A.V. Skripal', D.V. Ponomarev, E.V. Latysheva. *Semiconductors*, **50**, 1759 (2016). DOI: 10.1134/S1063782616130091
- [19] T.S. Bochkova, S.V. Igonin, D.A. Usanov, A.É. Postel'ga. *Russ. J. Nondestruct. Test.*, **54**, 576 (2018). DOI: 10.1134/S106183091808003X
- [20] K.S. Chemplin, D.B. Armstrong. *TIRI*, **50** (2), 272 (1962) (in Russian).
- [21] V.V. Nikol'skii. *Radiotekhnika i elektronika*, **2** (2), 157 (1957) (in Russian).
- [22] Yu.V. Egorov. *Chastichno zapolnennyye pryamougol'nye volnovody* (Sovetskoe radio, M., 1967) (in Russian).
- [23] A.H. Sihvola, J.A. Kong. *IEEE Transactions on Geoscience and Remote Sensing*, **26** (4), 420 (1988). DOI: 10.1109/36.3045
- [24] A. Katsounaros, K.Z. Rajab, Y. Hao, M. Mann, W.I. Milne. *Appl. Phys. Lett.*, **98**, 203105 (2011). DOI: 10.1063/1.359226
- [25] M. Mishra, S. Puthucheri, D. Singh. *IEEE Transactions on Magnetics*, **53** (8), 2800710 (2017). DOI: 10.1109/TMAG.2017.2698401
- [26] I.V. Lebedev. *Tekhnika i pribory SVCh* (Vysshaya shkola, M., 1970) (in Russian).

Translated by M. Shevelev